

## A simplified analysis of super building structures with setback

Hideo Takabatake<sup>1\*</sup>, Fumiya Ikarashi<sup>2</sup> and Motohiro Matsuoka<sup>2</sup>

<sup>1</sup>*Department of Architecture, Kanazawa Institute of Technology  
Institute of Disaster and Environmental Science 3-1 Yatsukaho, Hakusan, Ishikawa Prefecture, 924-0838, Japan*

<sup>2</sup>*Kanazawa Institute of Technology, 924-0838, Japan*

*(Received August 23, 2010, Accepted November 15, 2010)*

**Abstract.** One-dimensional rod theory is very effective as a simplified analytical approach to large scale or complicated structures such as high-rise buildings, in preliminary design stages. It replaces an original structure by a one-dimensional rod which has an equivalent stiffness in terms of global properties. The mechanical behavior of structures composed of distinct constituents of different stiffness such as coupled walls with opening is significantly governed by the local variation of stiffness. Furthermore, in structures with setback the distribution of the longitudinal stress behaves remarkable nonlinear behavior in the transverse-wise. So, the author proposed the two-dimensional rod theory as an extended version of the rod theory which accounts for the two-dimensional local variation of structural stiffness; viz, variation in the transverse direction as well as longitudinal stiffness distribution. This paper proposes how to deal with the two-dimensional rod theory for structures with setback. Validity of the proposed theory is confirmed by comparison with numerical results of computational tools in the cases of static, free vibration and forced vibration problems for various structures. The transverse-wise nonlinear distribution of the longitudinal stress due to the existence of setback is clarified to originate from the long distance from setback.

**Keywords:** simplified analytical method; extended rod theory; two-dimensional stiffness of structures; setback; nonlinear stress distribution; preliminary design for buildings; dynamic analysis.

---

### 1. Introduction

In order to carry out approximate analysis for a large scale complicated structure such as a high-rise building in the preliminary design stages, the use of equivalent rod theory is very effective. Rutenberg (1975), Smith and Coull (1991), and Tarjan and Kollar (2004) presented approximate calculations based on the continuum method, in which the building structure stiffened by an arbitrary combination of lateral load-resisting subsystems, such as shear walls, frames, coupled shear walls, and cores, are replaced by a continuum. Georgoussis (2006) proposed to assess frequencies of common structural bents including the effect of axial deformation in the column members for symmetrical buildings by means of a simple shear-flexure model based on the continuum approach. Tarian and Kollar (2004) presented the stiffnesses of the replaced sandwich

---

\* Corresponding author, Professor, E-mail: [hideo@neptune.kanazawa-it.ac.jp](mailto:hideo@neptune.kanazawa-it.ac.jp)

beam of the stiffening system of building structures.

Takabatake *et al.* (1993, 1995, 1996, 2001, 2005, 2006) developed a simple but accurate rod theory which takes account of longitudinal, bending, and transverse shear deformation, as well as shear-lag and demonstrated the effectiveness for various high-rise buildings, tube structures and mega structures.

The equivalent rod theory replaces the original structure by a model of one-dimensional rod with an equivalent stiffness distribution, appropriated with regard to the global behavior. Difficulty arises in this modeling due to the restricted number of freedom of the equivalent rod, because local properties of each structural member cannot always be properly represented, which leads to significant discrepancy in some cases. The one-dimensional idealization is able to deal only with the distribution of stiffness and mass in the longitudinal direction, possibly with an account of the averaged effects of transverse stiffness variation. Common practice structures are usually composed of a variety of members or structural parts, often including distinct constituents such as a frame-wall or coupled wall with opening. Overall behavior of such a structure is significantly affected by the local distribution of stiffness. In addition, the individual behavior of each structural member plays an important role from the standpoint of structural design.

So, the author (2010) proposed two-dimensional rod theory as an extension of the one-dimensional rod theory in order to take into account of the effect of transverse variations in individual member stiffness. Fig. 1 illustrates the difference between the one- and two-dimensional rod theories in evaluating the local stiffness distribution of structural components. In the two-dimensional approximation, structural components with different stiffness and mass distribution are continuously connected.

The exterior of tall buildings has frequently the shape with many setback parts. On such a building the local variation of stress is considered to be very remarkable due the existence of setback. This nonlinear phenomenon of stress distribution may be explained by two-dimensional rod theory but not by one-dimensional rod theory. In order to treat exactly the local stress variation due to setback, the proper boundary condition in the two-dimensional rod theory must separate into two

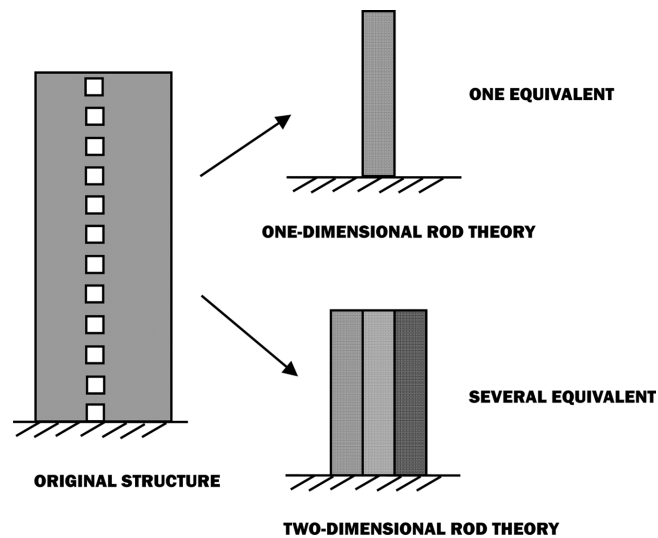


Fig. 1 The difference between one- and two-dimensional rod theories

parts. One part is the mechanical boundary condition corresponding to the setback part and the other is the continuous condition corresponding to longitudinally adjoining constituents. The previous paper proposed by the author (2010) demonstrated the governing equation but not how to formulate the two-dimensional rod theory to common structures with setback.

The aim of this paper is to prove the effectiveness of the two-dimensional rod theory to the general structures with setbacks. On the basis of the governing equation of the two-dimensional rod theory derived in the author's previous work (2010), this paper presents in detail the boundary conditions at the setback and clarifies the nonlinear behavior of longitudinal stress due to the existence of setback.

The Timoshenko beam theory is based on the assumption that the rotation of the cross section due to the transverse shear deformation takes account of the mean rotation of the longitudinal axis. The present two-dimensional rod theory agrees with the Timoshenko beam theory as selecting only the single frame part in the transverse direction. Since the Timoshenko beam theory falls considerably the number of variables, it is frequently employed in the one-dimensional rod theory for approximate analysis of building structures. However, it is necessary to clarify the effectiveness of the Timoshenko beam theory for the approximate analysis of building structures with setbacks. So, the nonlinear behavior of the longitudinal stresses due to the existence of setback is discussed from the results of numerical calculation for structural models with setback. The effectiveness of the theory proposed here is proven with regard to static, free vibration and forced vibration problems by comparison with the results based FEM code NASTRAN.

## 2. Survey of governing equation

Since in the previous paper proposed by author (2010) the governing equation of the two-dimensional rod theory presented in detail, this paper explains simply only the fundamental items which are necessary in the later development. For the sake of simplicity, we consider a two-dimensional structure of which the stiffness of constituents varies in the transverse-wise and longitudinal-wise. A Cartesian coordinate system  $x, y, z$ , as shown in Fig. 2, is employed, in which the axis  $x$  denotes the longitudinal axis, and the  $y$  and  $z$  the transverse axes. The coordinate axis  $x$  can be selected arbitrarily. For simplicity, the  $x$  axis is taken position in the left edge. Let us

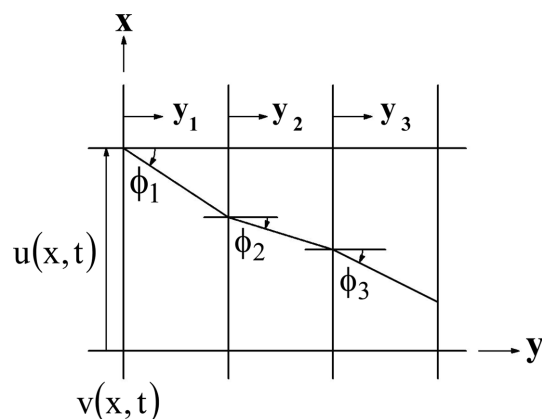


Fig. 2 Global coordinate system, local coordinate system, displacements and rotational angles

consider the structure composed of several structural parts with different stiffness. Each structural part is assumed to be parallel to the longitudinal axis  $x$  and to be transverse-wise homogeneous continuum in the cross section at a prescribed value of the longitudinal axis  $x$ . Also, each structural part connects continuously with the adjacent structural parts and satisfies the continuous condition for displacements. The number of the structural parts indicates ①, ②, ... in turn from the left hand side in the transverse direction. In order to assist the transverse axis  $y$ , each structural part has each local transverse axis  $y_i$  ( $i = 1, 2, 3, \dots, n$ ) which each original point is the left side of each structural part, as shown in Fig. 2.

The displacement components  $\overset{(i)}{U}(x, y, z, t)$ ,  $\overset{(i)}{V}(x, y, z, t)$ ,  $\overset{(i)}{W}(x, y, z, t)$  in the  $x$ -,  $y$ - and  $z$ -directions on the  $i$ -th structural part are expressed as

$$\overset{(i)}{U}(x, y, z, t) = u(x, t) - \sum_{k=1}^i y_k \phi_k(x, t) \quad (1)$$

$$\overset{(i)}{V}(x, y, z, t) = v(x, t) \quad (2)$$

$$\overset{(i)}{W}(x, y, z, t) = 0 \quad (3)$$

in which  $u(x, t)$  and  $v(x, t)$  are the longitudinal and transverse displacement components in the  $x$ - and  $y$ -directions on the axial point, respectively;  $\phi_i(x, t)$  is the rotational angle along the  $z$ -axis for the  $i$ -th structural part. The positive of these displacements takes for the positive value of the coordinate axis and the positive of the rotational angle  $\phi_i(x, t)$  takes for the clock wise along the positive  $z$ -axis. In Eq. (1) the following summation rule to simplify the expression is used for the  $i$ -th structural part

$$\sum_{k=1}^i y_k \phi_k = \sum_{k=1}^{i-1} \bar{y}_k \phi_k + y_i \phi_i \quad (4)$$

in which  $\bar{y}_k$  indicates the width of the  $k$ -th structural part.

Using the linear strain-displacement relation, the following expressions for the  $i$ -th structural part are obtained as

$$\overset{(i)}{\varepsilon}_x = \frac{\partial \overset{(i)}{U}}{\partial x} = u' - \sum_{k=1}^i y_k \phi_k' \quad (5)$$

$$\overset{(i)}{\gamma}_{xy} = \frac{\partial \overset{(i)}{U}}{\partial y_i} + \frac{\partial \overset{(i)}{V}}{\partial x} = -\phi_i + v' \quad (6)$$

$$\overset{(i)}{\gamma}_{xz} = \frac{\partial \overset{(i)}{U}}{\partial z} + \frac{\partial \overset{(i)}{W}}{\partial x} = 0 \quad (7)$$

in which primes indicate the differentiation with respect to  $x$ ;  $\overset{(i)}{\varepsilon}_x$  and  $\overset{(i)}{\gamma}_{xy}$  are longitudinal and shear strains on the  $i$ -th structural part, respectively.

Employing the well-known engineering stress-strain relationship, the stresses on the  $i$ -th structural part are written as

$$\sigma_x^{(i)} = E^{(i)} \varepsilon_x^{(i)} \quad (8)$$

$$\tau_{xy}^{(i)} = \kappa G^{(i)} \gamma_{xy}^{(i)} \quad (9)$$

in which  $E^{(i)}$  and  $G^{(i)}$  are the Young modulus and shear modulus on the  $i$ -th structural part;  $\kappa$  is the shear coefficient. The value of  $E^{(i)}$  and  $G^{(i)}$  may take independently on the  $i$ -th structural part and are given as replacing the original structure by an equivalent continuum, which are independent of Poisson's ratio  $\nu$ .

The governing equations of the two-dimensional rod theory is formulated by means of the Hamilton's principle. The equations of motion are given as

$$\delta u: \quad m\ddot{u} - (\rho S)_j \ddot{\phi}_j - (EAu')' + [(ES)_j \phi_j']' + C_u \dot{u} - P_x = 0 \quad (10)$$

$$\delta v: \quad m\ddot{v} - [(\kappa GA)v' - (\kappa GA)_j \phi_j']' + C_v \dot{v} - P_y = 0 \quad (11)$$

$$\delta \phi_k: \quad -(\rho S)_k \ddot{u} + (\rho I)_{kj} \ddot{\phi}_j + [(ES)_k u']' - [(EI)_{jk} \phi_j']' - (\kappa GA)_k v' + (\kappa GA)_k \phi_j \delta_k^j - (M)_k = 0 \quad (12)$$

in which the dot indicates differentiation with respect to time;  $\delta_k^j$  is Kronecker delta;  $\rho$  is mass density;  $m$  is mass per unit length;  $P_x$  and  $P_y$  are components of external loads in the  $x$ - and  $y$ -directions per unit length, respectively; and  $(M)_k$  is the component of moment around the  $z$ -axis per unit length acting on the  $k$ -th structural part;  $C_u$  and  $C_v$  are damping coefficients of two-dimensional rod. It must be noticed that since in the proposed theory the  $x$ -axis can be taken at an arbitrary point on the transverse cross section of the rod, the reduced equations of motion, as given by Eqs. (25) - (27), are in a coupled form.

The sectional stiffnesses for each structural part being homogeneous continuum with equivalent uniform thickness are defined as

$$A^{(i)} = \iint dy_i dz$$

$$S_k^{(i)} = \iint y_k dy_i dz \quad (13)$$

$$I_{kj}^{(i)} = \iint y_k y_j dy_i dz$$

in which  $A^{(i)}$ ,  $S_k^{(i)}$  and  $I_{kj}^{(i)}$  are the cross sectional area, the first and second inertia moments of the  $i$ -th structural part, respectively. In order to show concisely the sum of these sectional stiffness, we use the following notations in the governing equation

$$EA = \sum_{i=1}^n E A = E^{(1)} A^{(1)} + E^{(2)} A^{(2)} + \dots + E^{(n)} A^{(n)} \quad (14)$$

$$(ES)_k = \sum_{i=k}^n E^{(i)} S_k^{(i)} \quad (15)$$

$$(EI)_{kj} = \sum_{i=\max(k,j)}^n E I_{kj}^{(i)} \quad (16)$$

$$(\kappa GA)_i = \kappa G A^{(i)} \quad (17)$$

$$\kappa GA = \sum_{i=1}^n \kappa G A^{(i)} \quad (18)$$

in which the subscript  $i = \max(k,j)$  of  $\Sigma$  in Eq. (16) indicates that the integral  $i$  takes the maximum of  $k$  and  $j$ .

On the other hand, the boundary conditions are given as

$$EAu' - (ES)_j \phi'_j = \tilde{P}_x \quad \text{or } u = u^* \quad (19)$$

$$(\kappa GA)v' - (\kappa GA)_j \phi'_j = \tilde{P}_y \quad \text{or } v = v^* \quad (20)$$

$$-(ES)_k u' + (EI)_{jk} \phi'_j = (\tilde{m})_k \quad \text{or } \phi_k = \phi_k^* \quad (\text{for } k = 1, 2, 3, \dots, n) \quad (21)$$

in which  $\tilde{P}_x$  and  $\tilde{P}_y$  are external surface forces in the  $x$ - and  $y$ -directions at the mechanical boundary ( $x=l$ ), respectively, and  $(\tilde{m})_k$  is surface moment at the same point on the  $k$ -th structural part. Also,  $u^*$ ,  $v^*$ ,  $\phi_k^*$  are the prescribed longitudinal and transverse displacements, respectively, and the prescribed rotation on the  $i$ -th structural part at the geometrical boundary.

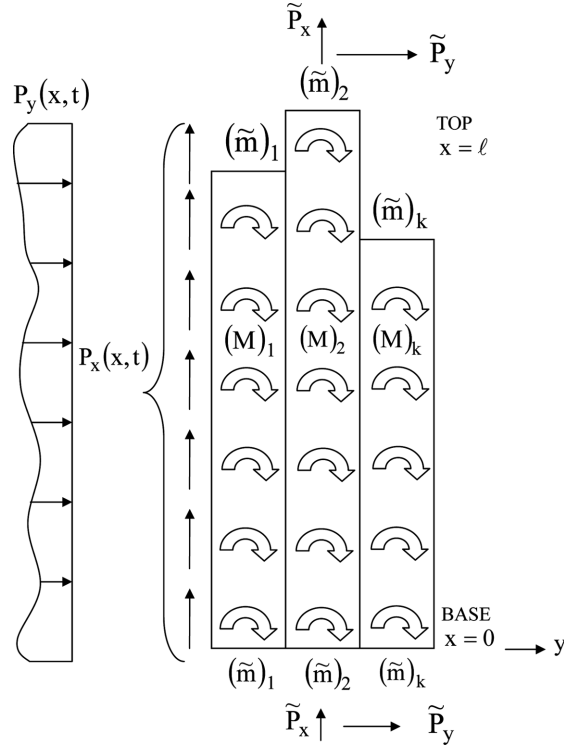


Fig. 3 External forces and external surface forces

### 3. Boundary conditions at setback

On the boundary with setback, the boundary conditions consists of two kind parts in which the one part is governed by the boundary condition corresponding to the setback part and the other part does by the continuous condition corresponding to longitudinally continuous structural parts. The boundary conditions for structural parts with setback part are expressed by the common boundary condition (21)<sub>i</sub>. On the other hand, the continuous condition corresponding to the longitudinally adjoining parts is considered as follows: In order to formulate continuous condition, the relationships between the stress resultants and the displacements are clarified from the following strain energy,  $U$

$$U = \frac{1}{2} \int_0^l \sum_{i=1}^n \iint \left[ \sigma_x^{(i)} \varepsilon_x^{(i)} + \tau_{xy}^{(i)} \tau_{xy}^{(i)} \right] dy_i dz dx \quad (22)$$

Substituting of Eq. (4) to Eq. (6) into Eq. (22), the strain energy expressed in term of stress resultants and stress couples is given as

$$U = \frac{1}{2} \int_0^l \left[ N \cdot u' + M_k \phi_k' - Q_k \phi_k + Q \cdot v' \right] dx \quad (23)$$

in which the stress resultants and stress couples are defined as

$$N \equiv \sum_{i=1}^n \iint \sigma^{(i)} dy_i dz \quad (24)$$

$$M_k \equiv - \sum_{i=k}^n \iint \sigma_x y_k^{(i)} dy_i dz \quad (25)$$

$$Q_i \equiv \iint \tau_{xy}^{(i)} dy_i dz \quad (26)$$

$$Q \equiv \sum_{i=1}^n Q_i \quad (27)$$

The variation of the strain energy in given from Eq. (23) becomes

$$\begin{aligned} \delta U = & \frac{1}{2} \int_0^l \left[ -N' \delta u - M_k' \delta \phi_k - Q_k \delta \phi_k - Q' \delta v \right] dx \\ & + [N \delta u]_{x=0}^{x=l} + [M_k \delta \phi_k]_{x=0}^{x=l} + [Q \delta v]_{x=0}^{x=l} \end{aligned} \quad (28)$$

It is clear from the above equation that the boundary conditions for longitudinally adjoining structural parts consist of the continuous conditions both for  $u$ ,  $v$ ,  $\phi_k$  and  $N$ ,  $Q$ ,  $M_k$ , respectively. These stress resultants may be expressed as

$$N = EAu' - (ES)_k \phi_k' \quad (29)$$

$$Q = (\kappa GA)v' - (\kappa GA)_j \phi_j' \quad (30)$$

$$M_k = -(ES)_k u' + (EI)_{kj} \phi_j' \quad (31)$$

The previous one-dimensional rod theory cannot expressed the local variation of stress due to the

existence of setback because the equivalent stiffness distribution appropriates with regard of the global behavior.

The continuous condition is formulated by virtually cutting the continuous structural parts excluded setback part. Thus, there are two kinds of continuous conditions for two cases without or with setback. The quantities corresponding to the left and right structural domains after virtually cutting the original structure discriminate with superscripts (A) and (B), respectively.

First, we consider a structure without setback, as shown in Fig. 4. Although this structure does not necessitate essentially virtual cutting, we investigate to examine the proposed continuous conditions for structures without setback. The finite difference method is employed for numerical computation. The accuracy of finite difference method depends on the use of a finer mesh and difference type. The central difference is higher in accuracy than the backward difference. However, when we treat

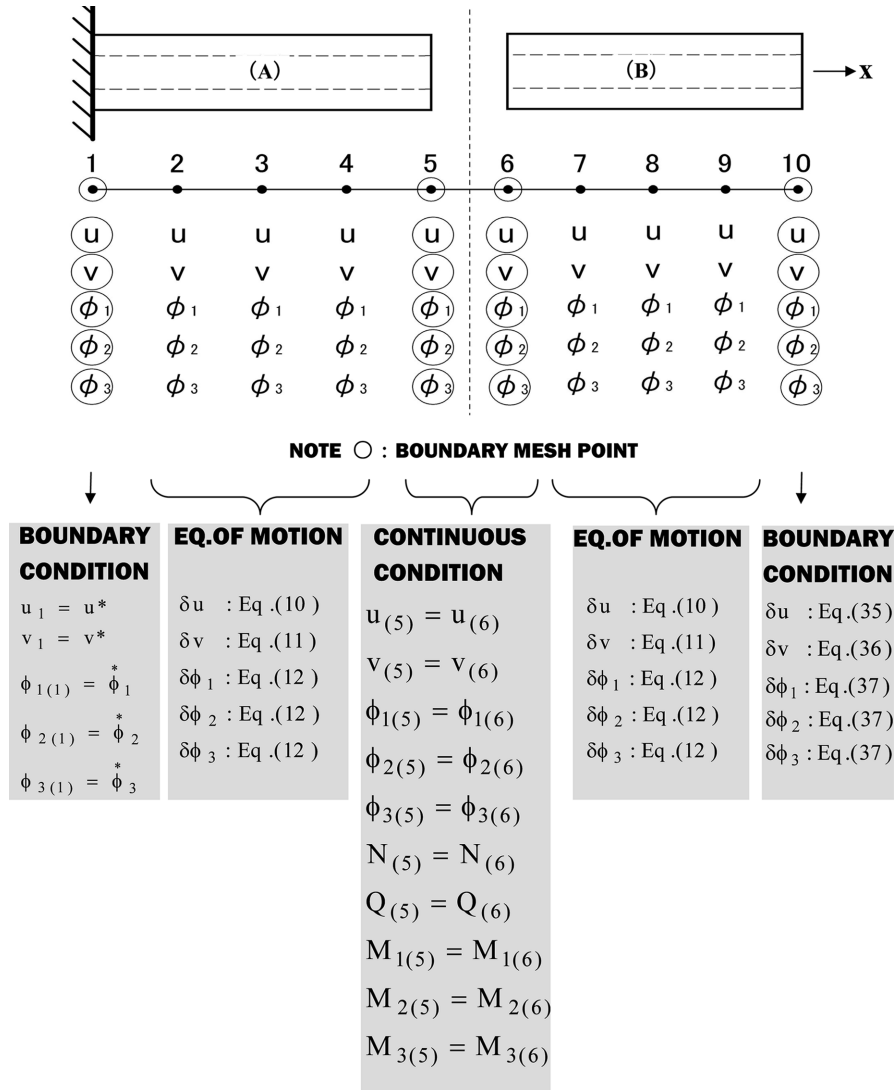


Fig. 4 Treatment of structures without setback

simultaneously the boundary condition including setback, the boundary condition consists of two kinds of boundary conditions on setback part and longitudinally adjoining parts. On the setback part the backward difference is advantageous. So, we use backward difference for the treatment of free boundary condition in order to avoid complicate and troublesome treatment. The recent progress of personal computer is aside from the increase of mesh points. Thus, the mesh points 1 and 10 become the boundary points at  $x=0$  and  $x=l$ , respectively. The mesh points 5 and 6 locate on the continuous point after virtually cutting and relate closely the continuous condition. The structure is considered to consist of three structure parts in the transverse-wise. Internal regular mesh points have 2, 3, and 4 for the left structural domain (A) and 7, 8, and 9 for the right structural domain (B). Since the structure has not setback, the structural part in the transverse-wise direction has the same number at the both structural domains. Hence there are the longitudinal displacement,  $u$ , transverse displacement,  $v$ , and the rotational angles,  $\phi_1$ ,  $\phi_2$  and  $\phi_3$ , at each internal mesh point. The equations of motion composed from Eq. (19) to Eq. (21) correspond to these displacements and rotational angles. Eq. (21) may take the value 1, 2, 3 for subscript  $k$ .

The boundary condition at  $x=0$  (base) become from Eq. (19)<sub>2</sub> to Eq. (21)<sub>2</sub> as

$$u = u^* \quad (32)$$

$$v = v^* \quad (33)$$

$$\phi_k = \phi_k^* \quad (\text{for } k = 1, 2, 3) \quad (34)$$

in which  $u^*$ ,  $v^*$  and  $\phi_k^*$  ( $k = 1, 2, 3$ ) are the prescribed displacements and rotational angles and they are zero for the clamped support.

Also, the free boundary condition at the top become from Eq. (19)<sub>1</sub> to Eq. (21)<sub>1</sub> as

$$EAu' - (ES)_j \phi'_j = \tilde{P}_x \quad (35)$$

$$(\kappa GA)v' - (\kappa GA)_j \phi_j = \tilde{P}_y \quad (36)$$

$$-(ES)_k u' + (EI)_{jk} \phi'_j = (\tilde{m})_k \quad (37)$$

The continuous condition may be written for the total 10 equations of the continuous conditions corresponding to the total 10 of  $u$ ,  $v$  and  $\phi_k$  ( $k = 1, 2, 3$ ) at the continuous mesh points 5 and 6. Specifically, the geometrical continuous conditions that the both corresponded displacement components at the mesh points 5 and 6 are identical become

$$u_{(5)} = u_{(6)} \quad (38)$$

$$v_{(5)} = v_{(6)} \quad (39)$$

$$\phi_{k(5)} = \phi_{k(6)} \quad (\text{for } k = 1, 2, 3) \quad (40)$$

and the mechanical continuous conditions that the both stress resultants and stress couples at the mesh points 5 and 6 are identical become

$$N_{(5)} = N_{(6)} \quad (41)$$

$$Q_{(5)} = Q_{(6)} \quad (42)$$

$$M_{k(5)} = M_{k(6)} \quad (\text{for } k = 1, 2, 3) \quad (43)$$

It must be noticed that  $N$  and  $Q$  are macro stress resultants for the whole cross section included all the structural parts but  $M_k$  are micro stress couples prescribed on each structural part.

Next, we consider the continuous condition for structures with setback, as shown in Fig. 5. This structure coexists the setback part and longitudinally continuous one at the surface cutting virtually. Therefore, two kinds of boundary condition at the location of setback are necessary. The structure is separated into two structural domains (A) and (B). The three structural parts in the transverse-wise are prepared. The structural domain (A) has three structural parts in which the second part joins the structural part at the separated structural domain (B). The statement concerning the mesh division is the same as the abovementioned explain, as shown in Fig. 4. The boundary conditions at the base ( $x = 0$ ) are the same as Eq. (32) to Eq. (34). The boundary conditions at the top ( $x = l$ ) are the same

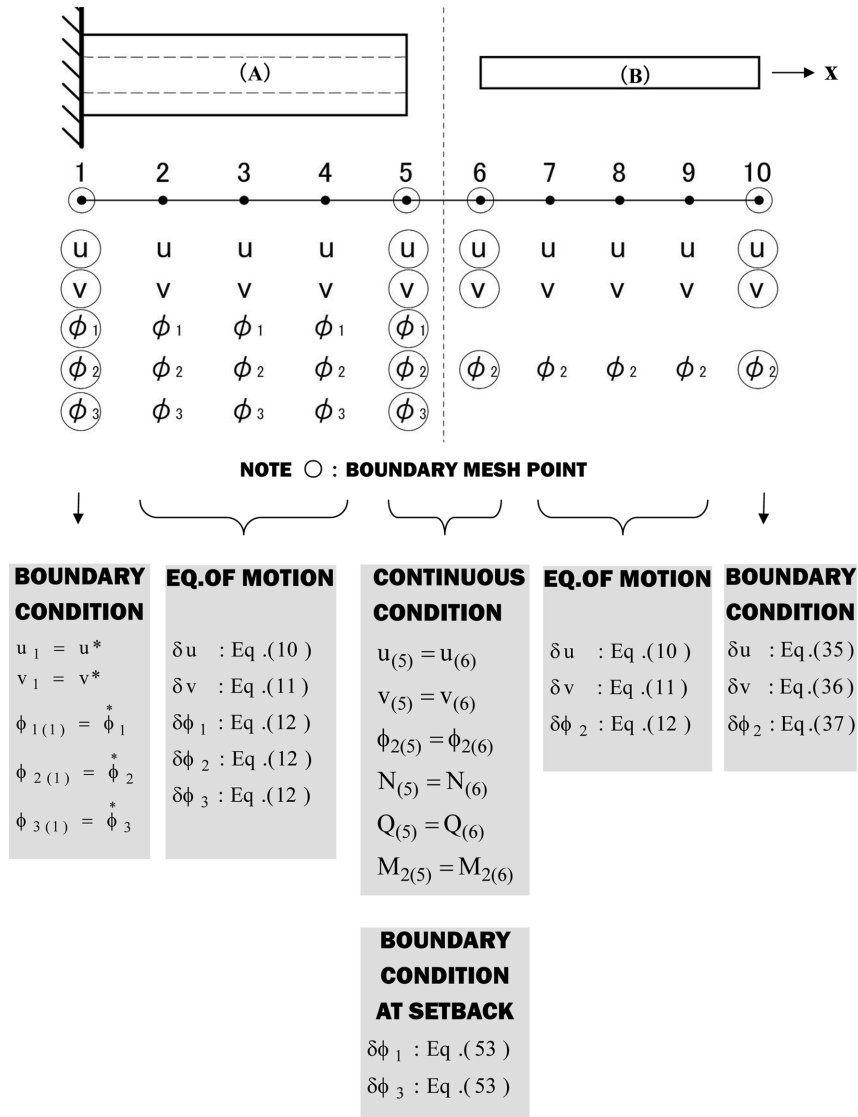


Fig. 5 Treatment of structures with setback

as Eq. (35) to Eq. (37) except for the effective of only the rotational angle  $\phi_2$  because of the existence of the structural part 2 in the domain (B).

$$EAu' - (ES)_2 \phi_2' = \tilde{P}_x \quad (44)$$

$$(\kappa GA)v' - (\kappa GA)_2 \phi_2 = \tilde{P}_y \quad (45)$$

$$-(ES)_2 u' + (EI)_{22} \phi_2' = (\tilde{m})_2 \quad (46)$$

The continuous conditions including the setback are considered as follows: The geometrical continuous conditions that the displacements and rotation equal to on the opposite face are

$$u_{(5)} = u_{(6)} \quad (47)$$

$$v_{(5)} = v_{(6)} \quad (48)$$

$$\phi_{2(5)} = \phi_{2(6)} \quad (49)$$

and the mechanical continuous condition that the stress resultants and stress couples equal to the opposite face become

$$N_{(5)} = N_{(6)} \quad (50)$$

$$Q_{(5)} = Q_{(6)} \quad (51)$$

$$M_{2(5)} = M_{2(6)} \quad (52)$$

In Eq. (47) to Eq. (52) the parenthesized subscript number indicates the mesh point. Furthermore, the mechanical boundary conditions corresponding at the mesh point 5 for the structural parts 1 and 3 at the setback in the domain (A) become

$$-(ES)_k u' + (EI)_{jk} \phi_j' = (\tilde{m})_k \quad (\text{for } k = 1, 3) \quad (53)$$

Hence the number of equations agrees with the one of variables. Although Eqs. (47) and (48) for the geometrical continuous conditions and Eqs. (50) and (51) for the mechanical continuous condition are the same as Eqs. (38), (39), (41) and (42), respectively, it must be noticed that Eqs. (49) and (52) are instead of Eqs. (40) and (43), respectively, due to the existence of setback.

#### **4. Expression of boundary conditions due to finite difference method**

When the numerical computation uses the finite difference method, the equation of motion effectuates on the internal mesh points, in which the variables concerning the boundary point must be replaced with variables concerning internal mesh points by means of the boundary conditions.

First, we present the free boundary condition at the top without setback, as given as Eq. (35) to Eq. (37). The displacement variable at the boundary point  $F$  is expressed with the adjacent mesh point  $F-1$ . Applying backward type for finite difference representation of derivatives to Eq. (35) to Eq. (37), we have in matrix terms

$$[A_F]\{u_F\} = [A_{F-1}]\{u_{F-1}\} + \{\tilde{P}\} \quad (54)$$

in which the matrixes  $[A_F]$  and  $[A_{F-1}]$  are defined as

$$[A_F] = \begin{bmatrix} \frac{EA}{\Delta x} & 0 & -\frac{(ES)_j}{\Delta x} \\ 0 & \frac{\kappa GA}{\Delta x} & -(\kappa GA)_j \\ -\frac{(ES)_k}{\Delta x} & 0 & \frac{(EI)_{jk}}{\Delta x} \end{bmatrix} (k=1,2,\dots) \quad (55)$$

$$[A_{F-1}] = \begin{bmatrix} \frac{EA}{\Delta x} & 0 & -\frac{(ES)_j}{\Delta x} \\ 0 & \frac{\kappa GA}{\Delta x} & 0 \\ -\frac{(ES)_k}{\Delta x} & 0 & \frac{(EI)_{jk}}{\Delta x} \end{bmatrix} (k=1,2,\dots) \quad (56)$$

$$\{u_F\} = \begin{Bmatrix} u_{(F)} \\ v_{(F)} \\ \phi_{j(F)} \end{Bmatrix} \quad (57)$$

$$\{u_{F-1}\} = \begin{Bmatrix} u_{(F-1)} \\ v_{(F-1)} \\ \phi_{j(F-1)} \end{Bmatrix} \quad (58)$$

$$\{\tilde{P}\} = \begin{Bmatrix} \tilde{P}_x \\ \tilde{P}_y \\ (\tilde{m})_k \end{Bmatrix} (k=1,2,\dots) \quad (59)$$

in which  $\Delta x$  is the mesh width. From Eq. (54) the variables at the boundary point  $F$  are expressed as

$$\{u_F\} = [A_F]^{-1}[A_{F-1}]\{u_{F-1}\} + [A_F]^{-1}\{\tilde{P}\} \quad (60)$$

Next, we represent the boundary conditions including setback, as shown in Fig. 6. Let us indicate the mesh points  $F$  and  $F+1$  which are located on the opposite surface at the setback due to virtual cutting, corresponding to the mesh points 5 and 6 in the structural domains (A) and (B), respectively, as shown in Fig. 5.

The structural parts at the mesh point  $F$  include both the rotational angles  $\phi_k$  corresponding to the structural parts with the setback, and the rotational angles  $\phi_k^*$  corresponding to the longitudinally

$j^*$  : NUMBER OF CONTINUOUS STRUCTURAL PARTS  
 $\hat{j}$  : NUMBER OF DISCONTINUOUS STRUCTURAL PARTS

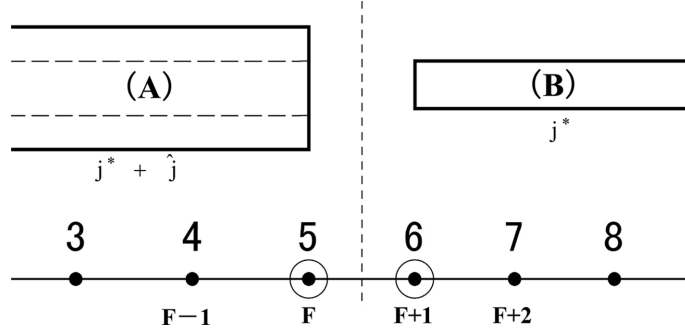


Fig. 6 Distinction between structural part with setback and continuous structural part

adjoining structural parts, in which the superscripts  $\wedge$  and  $*$  in subscript are introduced to distinguish the selected structural parts with setback and with continuity, respectively. The continuous conditions for the displacements and rotations at the continuous structural parts are

$$u_{(F)} = u_{(F+1)} \quad (61)$$

$$v_{(F)} = v_{(F+1)} \quad (62)$$

$$\phi_{k(F)}^* = \phi_{k(F+1)}^* \quad (63)$$

And the continuous conditions for stress resultants and stress couples become

$$N_{(F)} = N_{(F+1)} \quad (64)$$

$$Q_{(F)} = Q_{(F+1)} \quad (65)$$

$$M_{k(F)}^* = M_{k(F+1)}^* \quad (66)$$

On the other hand, the boundary conditions for the structural parts  $\hat{k}$  with setback are given from Eq. (53) as

$$-(ES)_{\hat{k}} u'_F + (EI)_{\hat{k},j_1} \phi'_{j_1,F} = (\tilde{m})_{\hat{k}} \quad (67)$$

Applying Eq. (29) to Eq. (31) into Eq. (64) to Eq. (66), we have

$$(EA) \cdot u'_F - (ES)_{j_1} \cdot \phi'_{j_1,F} = (EA) \cdot u'_{F+1} - (ES)_{j_2} \cdot \phi'_{j_2,F+1} \quad (68)$$

$$(\kappa GA) \cdot v'_F - (\kappa GA)_{j_1} \cdot \phi_{j_1,F} = (\kappa GA) \cdot v'_F - (\kappa GA)_{j_2} \cdot \phi_{j_2,F} \quad (69)$$

$$(ES)_{k^*} \cdot u'_F - (EI)_{k^*,j_1} \cdot \phi'_{j_1,F} = (ES)_{k^*} \cdot u'_F - (EI)_{k^*,j_2} \cdot \phi'_{j_2,F} \quad (70)$$

in which over-subscripts (A) and (B) indicate the values of structural domains (A) and (B), respectively.

The finite difference representation of derivatives to the structural domains (A) and (B) use the

backward and forward differences, respectively. It must be noticed that since the structural domains (A) and (B) are separated virtually at the portion with setback, the finite difference representation of derivatives across the two structural domains (A) and (B) cannot exist. Hence, the derivation in Eq. (67) uses the backward difference. Employing the relationships given from Eq. (61) to Eq. (63) into Eq. (68) to Eq. (70), the continuous conditions are given as

$$[A_F]\{u_F\} = [A_{F-1}]\{u_{F-1}\} + [A_{F+2}]\{u_{F+2}\} + \{\hat{P}\} \quad (71)$$

in which the matrixes  $[A_F]\{u_F\}$ ,  $[A_{F-1}]\{u_{F-1}\}$ ,  $[A_{F+2}]\{u_{F+2}\}$ ,  $\{\hat{P}\}$  are defined as

$$[A_F]\{u_F\} = \left[ \begin{array}{ccc|ccc} \begin{matrix} {}^{(A)}EA + {}^{(B)}EA \\ 0 \\ {}^{(A)}(ES)_{k^*} + {}^{(B)}(ES)_{k^*} \end{matrix} & 0 & \begin{matrix} {}^{(A)}\kappa GA \\ \Delta x \end{matrix} + \begin{matrix} {}^{(B)}\kappa GA \\ \Delta x \end{matrix} & \begin{matrix} -{}^{(A)}(ES)_{j^*} - {}^{(B)}(ES)_{j^*} \\ -({}^{(A)}\kappa GA)_{j^*} + ({}^{(B)}\kappa GA)_{j^*} \\ -{}^{(A)}(EI)_{k^*j^*} - {}^{(B)}(EI)_{k^*j^*} \end{matrix} & \begin{matrix} -{}^{(A)}(ES)_j \\ -({}^{(A)}\kappa GA)_j \\ -{}^{(A)}(EI)_{k^*j} \end{matrix} & \left\{ \begin{matrix} u_F \\ V_F \\ \phi_{j^*F} \end{matrix} \right\} \\ \hline -{}^{(A)}(ES)_{\hat{k}} & 0 & {}^{(A)}(EI)_{\hat{k}j^*} & {}^{(A)}(EI)_{\hat{k}j} & \left\{ \begin{matrix} \phi_{j^*F} \end{matrix} \right\} \end{array} \right] \quad (72)$$

$$[A_{F-1}]\{u_{F-1}\} = \left[ \begin{array}{ccc|ccc} \begin{matrix} {}^{(A)}EA \\ 0 \\ {}^{(A)}(ES)_{k^*} \end{matrix} & 0 & \begin{matrix} {}^{(A)}\kappa GA \\ \Delta x \end{matrix} & \begin{matrix} -{}^{(A)}(ES)_{j^*} \\ 0 \\ -{}^{(A)}(EI)_{k^*j^*} \end{matrix} & \begin{matrix} -{}^{(A)}(ES)_j \\ 0 \\ -{}^{(A)}(EI)_{k^*j} \end{matrix} & \left\{ \begin{matrix} u_{F-2} \\ V_{F-2} \\ \phi_{j^*F-2} \end{matrix} \right\} \\ \hline -{}^{(A)}(ES)_{\hat{k}} & 0 & {}^{(A)}(EI)_{\hat{k}j^*} & {}^{(A)}(EI)_{\hat{k}j} & \left\{ \begin{matrix} \phi_{j^*F-2} \end{matrix} \right\} \end{array} \right] \quad (73)$$

$$[A_{F+2}]\{u_{F+2}\} = \left[ \begin{array}{ccc|ccc} \begin{matrix} {}^{(B)}EA \\ 0 \\ {}^{(B)}(ES)_{k^*} \end{matrix} & 0 & \begin{matrix} {}^{(B)}\kappa GA \\ \Delta x \end{matrix} & \begin{matrix} -{}^{(B)}(ES)_{j^*} \\ 0 \\ -{}^{(B)}(EI)_{k^*j^*} \end{matrix} & \begin{matrix} 0 \\ 0 \\ 0 \end{matrix} & \left\{ \begin{matrix} u_{F+2} \\ V_{F+2} \\ \phi_{j^*F+2} \end{matrix} \right\} \\ \hline 0 & 0 & 0 & 0 & \left\{ \begin{matrix} \phi_{j^*F+2} \end{matrix} \right\} \end{array} \right] \quad (74)$$

$$\{\hat{P}\} = \left\{ \begin{matrix} 0 \\ 0 \\ 0 \\ \tilde{m}_k \Delta x \end{matrix} \right\} \quad (75)$$

Solving Eq. (71) for  $\{u_F\}$ , we have

$$\{u_F\} = [A_F]^{-1}[A_{F-1}]\{u_{F-1}\} + [A_F]^{-1}[A_{F+2}]\{u_{F+2}\} + [A_F]^{-1}\{\hat{P}\} \quad (76)$$

Thus the variables at the boundary mesh point  $F$  have been replaced with the variables at the adjacent mesh points  $F - 1$  and  $F + 2$ .

## 5. Boundary conditions for free vibrations

The boundary conditions at free edge for the free vibrations are given from neglecting the boundary forces in Eq. (19) to Eq. (21) as

$$EAu' - (ES)_j\phi'_j = 0 \quad (77)$$

$$(\kappa GA)v' - (\kappa GA)_j\phi_j = 0 \quad (78)$$

$$-(ES)_k u' + (EI)_{jk}\phi'_j = 0 \quad (79)$$

The method of separation of variables is employed assuming that

$$u(x, t) = \bar{u}(x)e^{i\omega t} \quad (80)$$

$$v(x, t) = \bar{v}(x)e^{i\omega t} \quad (81)$$

$$\phi_j(x, t) = \bar{\phi}_j(x)e^{i\omega t} \quad (82)$$

in which  $\bar{u}(x)$ ,  $\bar{v}(x)$ ,  $\bar{\phi}_j(x)$ , are function of  $x$ . Applying Eq. (80) to Eq. (82) into Eq. (77) to Eq. (79) and solving for  $\{\bar{u}_F\}$ , we have

$$\{\bar{u}_F\} = [A_F]^{-1}[A_{F-1}]\{\bar{u}_{F-1}\} \quad (83)$$

Thus, we can easily use from the modification of the boundary conditions for the static problem.

## 6. Boundary conditions for forced vibrations

Let us consider the boundary condition at the free edges, subjected to forced vibrations. The relationships between the incremental quantities at time  $t$  and  $t + \Delta t$  in which  $\Delta t$  is diminutive incremental time, may be written as

$$u(t + \Delta t) = u(t) + \Delta u \quad (84)$$

$$v(t + \Delta t) = v(t) + \Delta v \quad (85)$$

$$\phi_j(t + \Delta t) = \phi_j(t) + \Delta \phi_j \quad (86)$$

Neglecting the variation of the cross sectional stiffness at the diminutive incremental time, the boundary conditions in the incremental expression may be

$$EA\Delta u' - (ES)_j\Delta\phi'_j = \Delta\tilde{P}_x \quad (87)$$

$$(\kappa GA)\Delta v' - (\kappa GA)_j\Delta\phi_j = \Delta\tilde{P}_y \quad (88)$$

$$-(ES)_k\Delta u' + (EI)_{jk}\Delta\phi'_j = \Delta(\tilde{m})_k \quad (89)$$

in which  $\Delta\tilde{P}_x$ ,  $\Delta\tilde{P}_y$ , and  $\Delta(\tilde{m})_k$  are indicate incremental external surface loads. The above equations essentially are the same expression as Eq. (19)<sub>1</sub> to Eq. (21)<sub>1</sub>. The reduced expressions for incremental displacements and rotations at the boundary mesh point may be expressed with Eq. (54).

## 7. Numerical results

The two-dimensional rod theory replaces an original structure composed of various structural stiffnesses in the transverse-wise with many continuous structural parts in which each constituent is uniform transverse stiffness. In this paper the numerical computation considers structures with setback, but the stiffness is arbitrarily variable in the longitudinal and transverse directions. We use the finite difference method in the numerical computation.

Now, the boundary conditions are assumed to be clamped at the base and free at the top and that the surface loads are inexistence at the setback and top.

The exactness of the two-dimensional rod theory proposed here is proven through a comparison of numerical results obtained from the proposed theory and FEM code NASTRAN for numerical models. The calculation in FEM is obtained from applying usual shell elements to the numerical models used here. After confirming the convergence of numerical results, the number of the division for the mesh size of the shell element takes 14 in the transverse-wise and 50 in the longitudinal-wise. The numerical models are proposed the four types of MODEL-1N, MODEL-2N, MODEL-1V, and MODEL-2V, as shown in Figs. 7 to 8. These models include two types of setback and two types of the variation of transverse-wise stiffness. These models have one setback at 15m height and the total height is 25 m and the width at the base ( $x=0$ ) is 7 m. MODEL-1N and MODEL-2N have the uniform stiffness in which the Young modulus  $E = 2.06 \times 10^{11}$  N/m<sup>2</sup>, the shear modulus  $G = 7.92 \times 10^{10}$  N/m<sup>2</sup>, mass density  $\rho = 7850$  kg/m<sup>3</sup>. MODEL-1N and MODEL-1V have the same setback but the Young modulus of the central structural part in MODEL-1V is twice stronger than the other structural parts. Similarly, the width after setback in MODEL-2N and MODEL-2V is smaller than the MODEL-1N and MODEL-2V. These models are regarded as two-dimensional continuum after replacing appropriately a frame with two-dimensional continuum.

Figs. 9(a) and 9(b) show the distribution of the lateral displacements subjected to static uniform lateral load 40N/m. Since all numerical models have setback at the height of 15 m, the transverse-wise distribution of the longitudinal stress  $\sigma_x$  depart remarkably from the linear distribution as the height  $x$  approaches to the setback. Figs. 10(a) to 10(d) show the transverse-wise distribution of the longitudinal stress  $\sigma_x$  at height varied from 11 to 15 m per unit meter. Although the hypothesis which the transverse-wise distribution of the longitudinal stress is linear may apply approximately reasonable until 11 m, it becomes remarkable nonlinear as approach to the setback. On the other

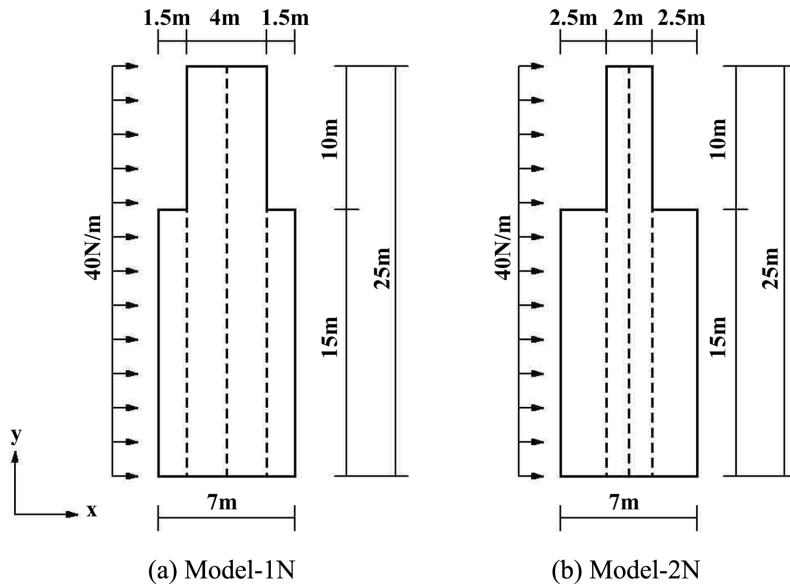


Fig. 7 Numerical models: (a) Model-1N and (b) Model-2N

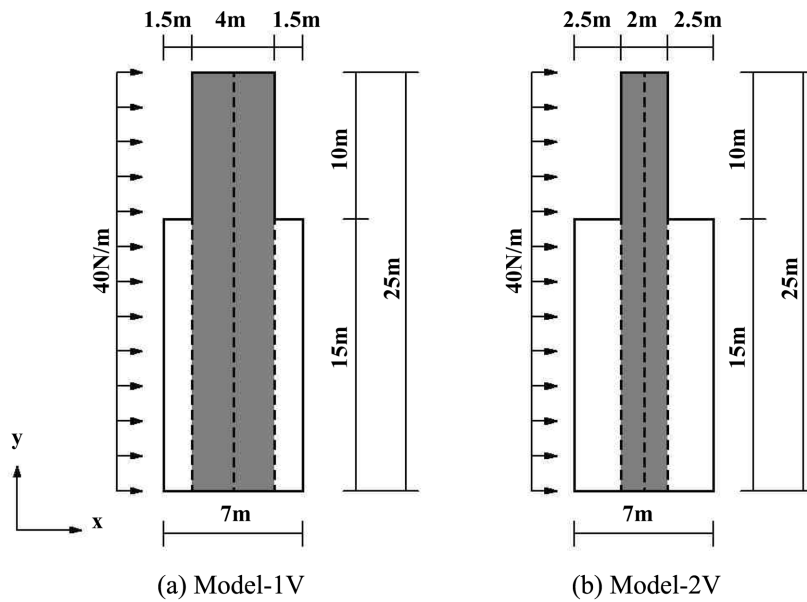


Fig. 8 Numerical models: (a) Model-1V and (b) Model-2V

hand, the distribution of  $\sigma_x$  at the height over setback is remarkable nonlinear, as shown in Figs. 11(a) and 11(b). Figs. 12 and 13 compare about the distribution of longitudinal stresses at 13 m and 15 m in height with the both results obtained from the present theory and FEM. The good agreement between analytical calculations and FEM code NASTRAN in the shell element is confirmed for the displacements and stress. The nonlinear stress behavior is more remarkable in MODEL-1V and MODEL-2V with variable stiffness than in MODEL-1N and MODEL-2N with uniform stiffness. The occurrence of nonlinear behavior of the longitudinal stress is greater in

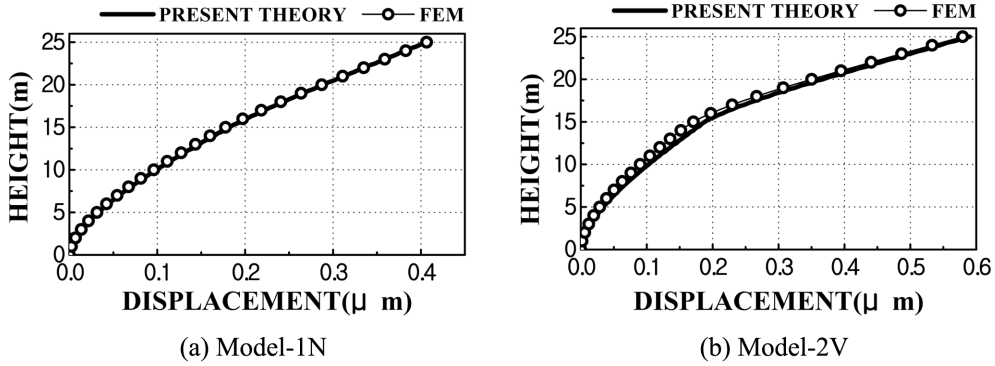


Fig. 9 Static lateral displacement: (a) Model-1N and (b) Model-2V

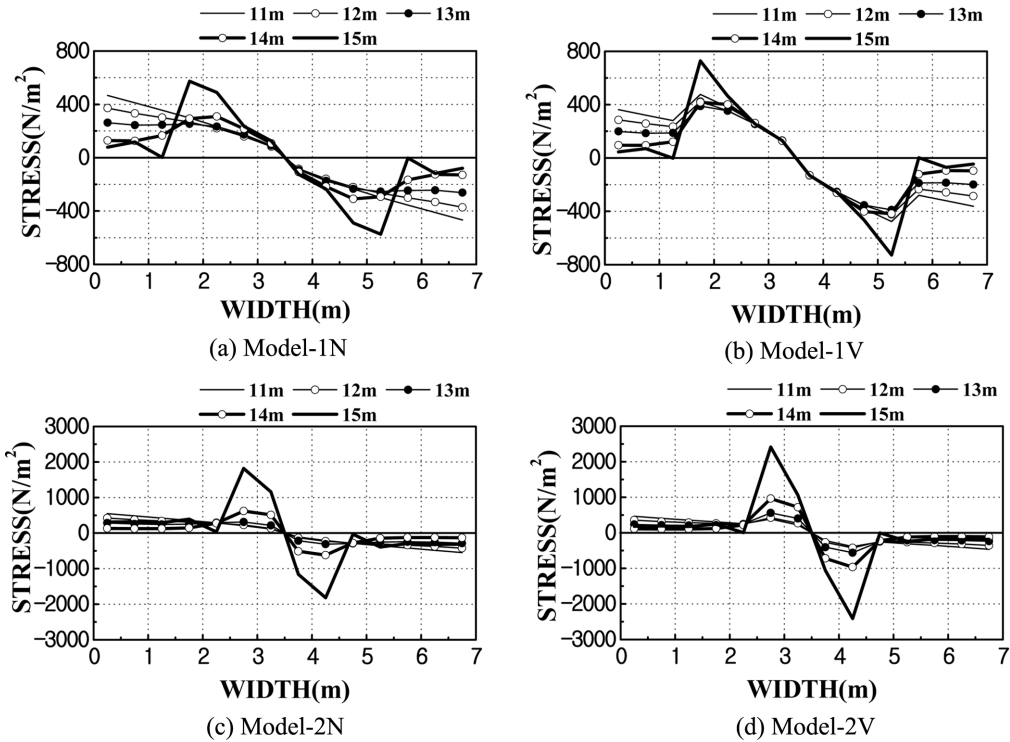


Fig. 10 Longitudinal stress distributions at each height from 11 to 15 m: (a) Model-1N, (b) Model-1V, (c) Model-2N and (d) Model-2V

MODEL-2N and MODEL-2V than in MODEL-1N and MODEL-1V. The influence of nonlinear stress distribution is remarkable as the width of setback increases.

The remarkable nonlinear of stress distribution near the setback is based on the boundary condition that the longitudinal stress must be zero on the part at the setback. The continuous condition for the moment is effective on only the continuous parts, corresponding to Eq. (52). The continuous condition for the moment on the one-dimensional rod theory considers for the total transverse cross section without distinction of setback. However, the current two-dimensional rod

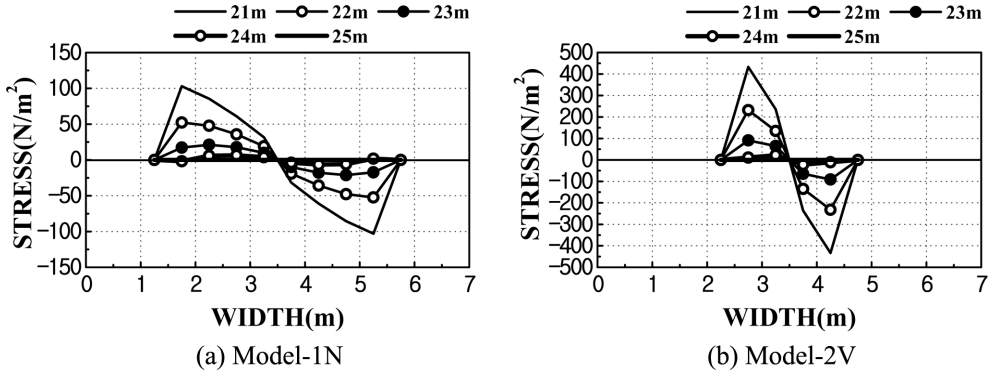


Fig. 11 Longitudinal stress distributions at each height from 21 to 25 m: (a) Model-1N and (b) Model-2V

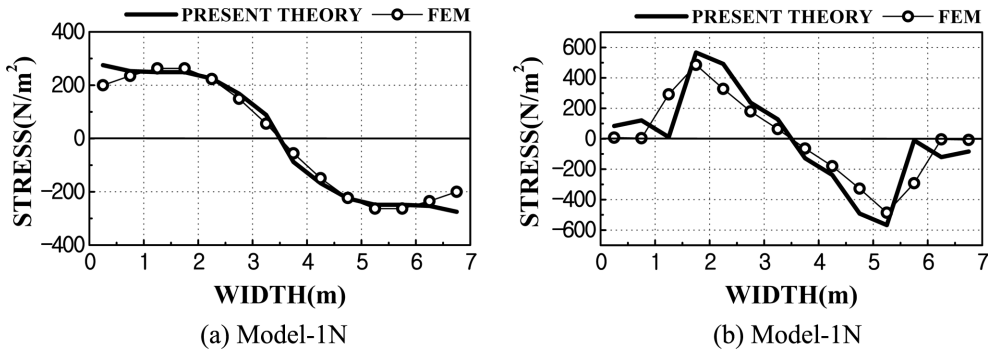


Fig. 12 Longitudinal stress distribution of Model-1N: (a) at 13 m height and (b) at 15 m height

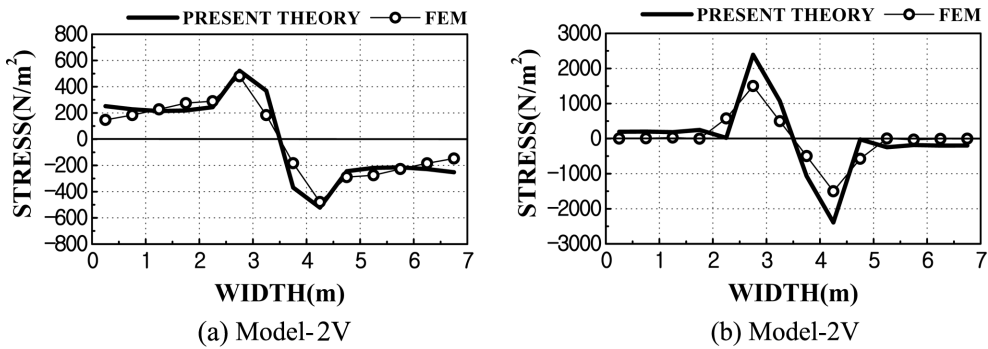


Fig. 13 Longitudinal stress distribution of Model-2V: (a) at 13 m height and (b) at 15 m height

theory distinguishes exactly, as given in Eq. (46) for the continuous part and Eq. (53) for the setback part. Thus, the two-dimensional rod theory may obtain the nonlinear stress distribution.

Next, we indicate numerical result from the transverse free vibration. Table 1 indicates the natural frequencies as compared with the present theory and FEM. Fig. 14 shows the relationships of numerical results between the present theory and FEM for the first to fifth natural modes. Similarly, Fig. 15 presents participation functions corresponding to the first to third natural modes.

Last, we consider the forced vibration subjected to earthquake wave EL-CENTRO 1940 NS at the

Table 1 Relationships between the present theory and FEM for natural frequency(rad/sec)

| Model     | Mode | ① Present theory | ② FEM   | Ratio ① / ② |
|-----------|------|------------------|---------|-------------|
| MODEL -1N | 1st  | 67.43            | 66.90   | 1.01        |
|           | 2nd  | 232.08           | 229.53  | 1.01        |
|           | 3rd  | 517.25           | 522.58  | 0.99        |
|           | 4th  | 880.39           | 867.86  | 1.01        |
|           | 5th  | 1244.90          | 1219.35 | 1.02        |
| MODEL -2V | 1st  | 79.21            | 79.29   | 1.00        |
|           | 2nd  | 189.84           | 189.25  | 1.00        |
|           | 3rd  | 543.59           | 541.57  | 1.00        |
|           | 4th  | 839.95           | 802.00  | 1.05        |
|           | 5th  | 1275.20          | 1281.75 | 0.99        |

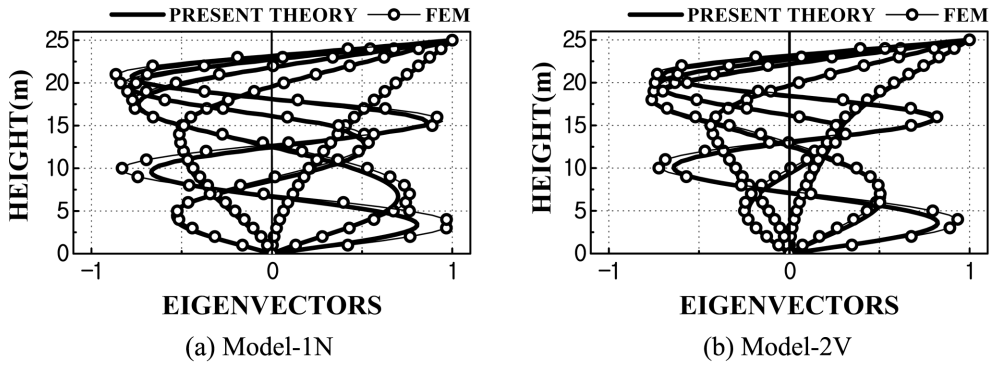


Fig. 14 Natural mode of lateral free vibration: (a) Model-1N and (b) Model-2V

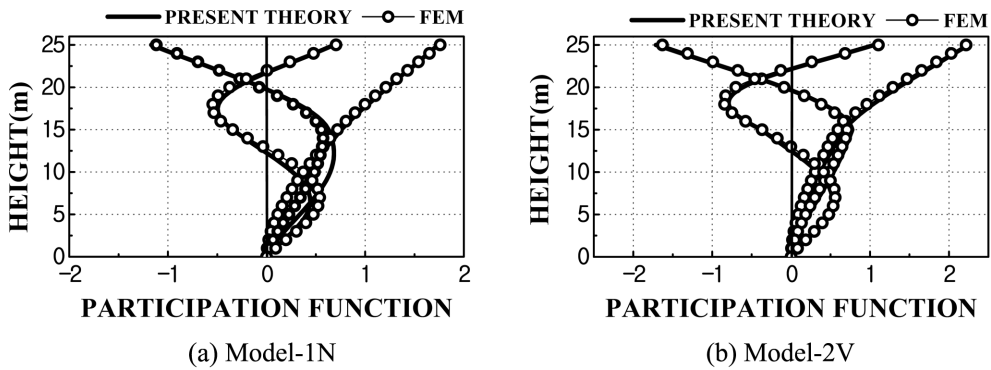


Fig. 15 Participation functions of lateral free vibration: (a) Model-1N and (b) Model-2V

base. The damping ratio is  $h_1 = 0.02$  for the first mode and  $h_n = h_1 \omega_n / \omega_1$  for the  $n$ -th higher damping ratio. Figs. 16 to 18 indicate the distributions of maximum lateral displacement, transverse shear, overturning moment, respectively. The numerical results show the good agreement between the proposed theory and FEM.

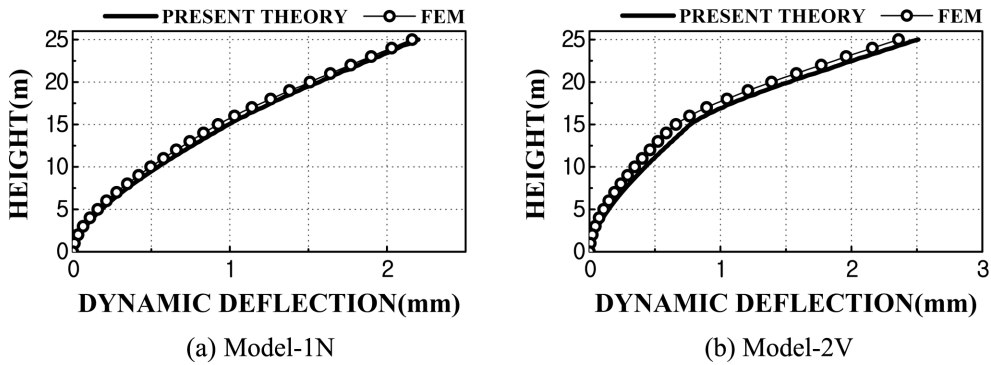


Fig. 16 Maximum dynamic lateral deflection: (a) Model-1N and (b) Model-2V

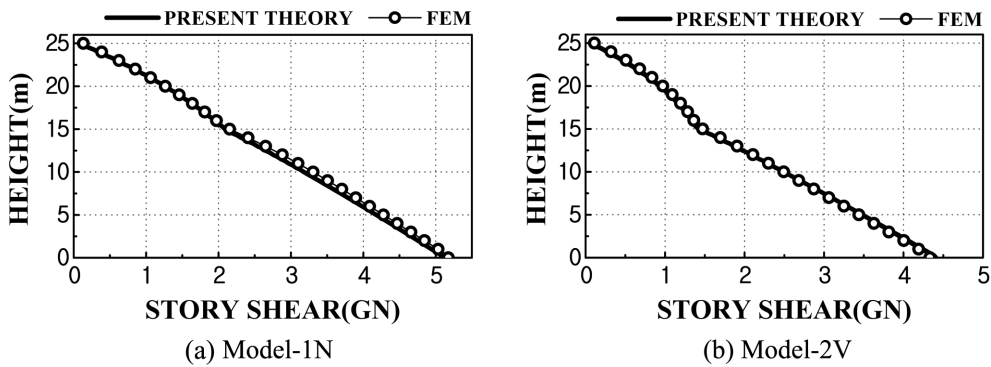


Fig. 17 Maximum dynamic story shear: (a) Model-1N and (b) Model-2V

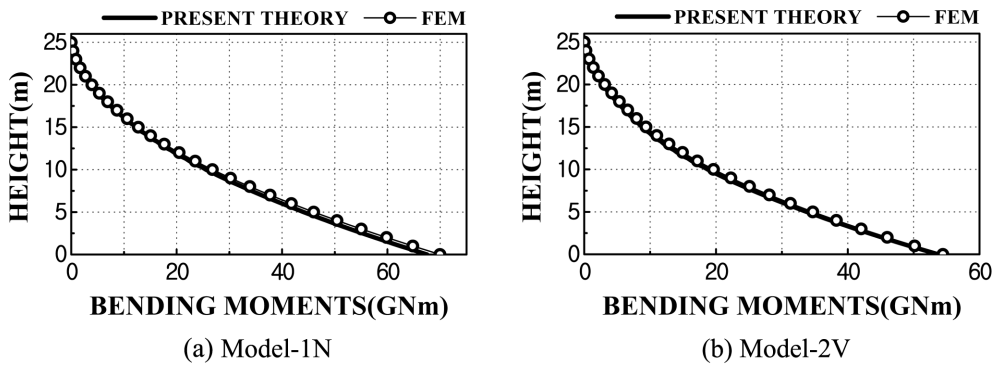


Fig. 18 Maximum bending moment: (a) Model-1N and (b) Model-2V

## 8. Conclusions

Two-dimensional rod theory has been presented for simply analyzing a large or complicated structure with setback in which the stiffness and mass due to the existence of setback vary rapidly in the longitudinal and transverse directions. The effectiveness of this theory has been demonstrated from numerical results for exemplified numerical models. The transverse-wise distribution of longitudinal stress for structures with setbacks has been clarified to behave remarkable nonlinear

behavior. Since the structural form of high-rise buildings with setbacks is frequently adapted in the world, the incensement of stress distribution occurred locally due to setback is very important for structural designers. The present theory may estimate such nonlinear stress behaviors in the preliminary design stages. The further development of the present theory will be necessary to extend to the three-dimensional rod theory which is applicable to a complicated building with three dimensional behavior due to the eccentric station of many earthquake-resistant structural members, such as shear walls with opening.

## Acknowledgments

This research is supported by Grant-in-Aid for Scientific Research in Japan.

## References

- Buchholdt, H. (1997), *Structural dynamics for engineers*, Thomas Telford.
- Georgoussis, G.K. (2006), "A simple model for assessing periods of vibration and modal response quantities in symmetrical buildings", *Struct. Des. Tall. Spec.*, **15**(2), 139-151.
- Pübal, Z. (1988), *Theory and calculation of frame structures with stiffening walls*, Elsevier, Amsterdam.
- Rutenberg, A. (1975), "Approximate natural frequencies for coupled shear walls", *Earth. Eng. Struct. Dyn.*, **4**(1), 95-100.
- Smith, B.S. and Coull, A. (1991), *Tall building structures: analysis and design*, John Wiley & Sons, New York.
- Scarlet, A.S. (1996), *Approximate methods in structural seismic design*, E&FN Spon.
- Takabatake, H. and Matsuoka, O. (1983), "The elastic theory of thin-walled open cross sections with local deformations", *Int. J. Solids Struct.*, **19**(12), 1065-1088.
- Takabatake, H. and Matsuoka, O. (1987), "Elastic analyses of circular cylindrical shells by rod theory including distortion of cross section", *Int. J. Solids Struct.*, **23**(6), 797-817.
- Takabatake, H. Mukai, H. and Hirano, T. (1993), "Doubly symmetric tube structures: I: static analysis", *J. Struct. Eng. - ASCE*, **119**(7), 1981-2001.
- Takabatake, H. Mukai, H. and Hirano, T. (1993), "Doubly symmetric tube structures: II: dynamic analysis", *J. Struct. Eng. - ASCE*, **119**(7), 2002-2016.
- Takabatake, H. Takesako, R. and Kobayashi, M. (1995), "A simplified analysis of doubly symmetric tube structures", *Struct. Des. Tall Build.*, **4**(2), 137-153.
- Takabatake, H. (1996), "A simplified analysis of doubly symmetric tube structures by the finite difference method", *Struct. Des. Tall Build.*, **5**(2), 111-128.
- Takabatake, H. and Nonaka, T. (2001), "Numerical study of Ashiyahama residential building damage in the Kobe Earthquake", *Earth. Eng. Struct. Dyn.*, **30**(6), 879-897.
- Takabatake, H. Nonaka, T. and Tanaki, T. (2005), "Numerical study of fracture propagating through column and brace of Ashiyahama residential building in Kobe Earthquake", *Struct. Des. Tall. Spec.*, **14**(2), 91-105.
- Takabatake, H. and Satoh, T. (2006), "A simplified analysis and vibration control to super-high-rise buildings", *Struct. Des. Tall. Spec.*, **15**(4), 363-390.
- Takabatake, H. (2010), "Two-dimensional rod theory for approximate analysis of building structures", *Earthq. Struct.*, **1**(1), 1-19.
- Tarjian, G. and Kollar, L.P. (2004), "Approximate analysis of building structures with identical stories subjected to earthquake", *Int. J. Solids Struct.*, **41**(5), 1411-1433.